Electronic Transduction of HIV-1 Drug Resistance in AIDS Patients

Lital Alfonta,[a, c] Immanuel Blumenzweig,[b] Maya Zayats,[a] Lea Baraz,[b] Moshe Kotler,*[b] and Itamar Willner*[a]

A drug composition consisting of nucleoside reverse transcriptase inhibitors (NRTIs), non-nucleoside reverse transcriptase inhibitors (NNRTIs), and protease inhibitors (PIs) is commonly used in AIDS therapy. A major difficulty encountered with the therapeutic composite involves the emergence of drug-resistant viruses, especially to the PIs, regarded as the most effective drugs in the composition. We present a novel bioelectronic means to detect the appearance of mutated HIV-1 exhibiting drug resistance to the PI saquinavir. The method is based on the translation of viral RNA, the association of cleaved or uncleaved Gag polyproteins at an electrode surface functionalized with the respective antibodies, and the bioelectronic detection of the Gag polyproteins associated with the surface. The bioelectronic process includes the association of anti-MA or anti-CA antibodies, the secondary binding of an antibody–horseradish peroxidase (HRP) conjugate, and the biocatalyzed precipitation of an insoluble product on the electronic transducers. Faradaic impedance measurements and quartz crystal microbalance analyses are employed to follow the autoprocessing of the Gag polyproteins. The method was applied to determine drug resistance in infected cultured cells and also in blood samples of consenting AIDS patients. The method described here is also applicable to the determination of drug effectiveness in AIDS patients and to screening of the efficiency of newly developed drugs.

Introduction

The currently used methodology to detect drug-resistant viruses in AIDS patients consists principally of phenotyping and genotyping viruses isolated from blood samples.[1] Phenotyping of the viral protease (PR) is carried out through the isolation and propagation of viruses in cultured cells in the presence of anti-HIV drugs,[2] or by the cloning and expression of the viral PR in bacterial cells, and assessment of the enzyme activity in the presence of protease inhibitors (PIs).[3] Nonetheless, the virus-propagation step in the presence of the PI may itself result in the growth of mutated viruses[4,5] that do not reflect the initial mutants of the HIV carrier. In addition, sequencing of the PR-encoding region in the viral RNA is used to genotype the drug resistance characteristic of the virus.[6,7] The sequencing of the viral genome is only partially representative, since only a limited number of viral DNA molecules are analyzed. Thus, although significant advances in the detection of HIV drug resistance have been accomplished, the different methods exhibit drawbacks, and the development of analytical methods that bypass the virus-propagation step of the analyzed samples would be advantageous.

The retroviral Gag and Gag-Pol polyproteins are translated from mRNA that is indistinguishable from the full-length genomic RNA found in virions. The ratio of HIV Gag to Gag-Pol polyprotein expression is approximately 20:1.[8] The viral Gag and Gag-Pol polyproteins are processed by a virus-encoded PR, that consists of a dimer composed of two identical subunits.[9] Cleavage of the viral polyproteins is a key step in viral maturation, and without specific cleavage of the precursors, the virion is not infectious.[10–12] Previous studies have indicated that PR is already active in its Gag-Pol precursor form, and that the cleavage of the polyproteins may occur by inter- or intramolecular mechanisms.[13–15] HIV PR inhibitors are effective against wild-type HIV both in vitro and in vivo, but are also rapidly selected for HIV variants displaying reduced susceptibility to the PR inhibitors.[16,17] Currently, all of the clinically approved inhibitors of HIV PR are peptide mimetics that interact with the protease active site and adjacent substrate specificity pockets. Mutations both in these regions and in distal sites affect the inhibitor and substrate binding by altering the number and/or strength of subsite interactions.[18] Consequently, in the presence of a PR inhibitor, there is a replicative advantage for HIV-containing mutations that decrease affinity to the inhibitor while retaining sufficient enzyme activity to process the Gag and Gag-Pol polyproteins.

Bioelectronics, and specifically the development of biosensors, is a rapidly developing research field.[19,20] Electronic biosensors transduce biorecognition events into electronic signals. Electrodes,[21] piezoelectric crystals,[22] and field-effect transistors[23] are often used as electronic transduction units. Electrochemical transduction of enzyme–substrate interactions[21] and

[a] *Dr. L. Alfonta, M. Zayats, Prof. Dr. I. Willner*
Institute of Chemistry, The Hebrew University of Jerusalem
Jerusalem 91904 (Israel)
Fax: (+972) 2-6527715
E-mail: willnea@vms.huji.ac.il

[b] *I. Blumenzweig, L. Baraz, Prof. Dr. M. Kotler*
Department of Pathology, The Hebrew University–Hadassah Medical School
Jerusalem 91120 (Israel)
E-mail: mkotler@cc.huji.ac.il

[c] *Dr. L. Alfonta*
Current address:
Department of Chemistry, The Scripps Research Institute
10550 North Torrey Pines Road, La Jolla, California 92037 (USA)

 DOI: 10.1002/cbic.200400009

of antigen–antibody[24] or nucleic acid–DNA[25,26] recognition processes has been accomplished. Microgravimetric quartz-crystal microbalance measurements have been employed for the detection of antigens[22] or DNA,[27] and field-effect transistors have been used to analyze antibody–antigen complexes.[23] Recent efforts in bioelectronics have been directed towards amplified detection of antigen–antibody[28] or nucleic acid–DNA interactions.[29–31] The replication of the analyzed DNA to yield a redox-active replica coupled to a bioelectrocatalytic cascade,[29] or the conjugation of nucleic acid-labeled particulate systems such as liposomes[30] or nanoparticles[31] have been used to amplify DNA detection processes. A powerful method to amplify antigen–antibody or DNA (RNA) detection involved the coupling of a biocatalytic conjugate to the biorecognition complex; this resulted in the precipitation of an insoluble product on electronic transducers.[28,32] The insulation of the electrodes by the insoluble product or the increase in the mass associated with piezoelectric crystals as a result of the formation of the precipitate was electronically transduced. Here we report on the amplified detection of in vitro translation of viral mRNA. To the best of our knowledge, this is the first example of an electronic device that transduces an mRNA translation process. Specifically, we describe the electronic transduction, through an in vitro mRNA-translation process, of drug resistance developed in HIV-1 carriers. The method not only enables the diagnosis of drug-resistant HIV-1, but also the identification of the most efficient drugs for antiviral therapy and the rapid screening of new anti-HIV-1 drugs.

Results and Discussion

In vitro translation of viral RNA results in the synthesis of precursors being autoprocessed by the translated protease. The bioelectronic method enables us to compare the processing efficiency by comparing the amounts of viral precursors cleaved and not cleaved by the intrinsic protease. Scheme 1 illustrates the method of probing HIV drug resistance by analysis of the PR inhibition. The electronic transducers (Au electrodes or Au–quartz crystals) are modified with protein G, which binds the anti-CA-Ab. Inhibition of the protease activity results in the binding of uncleaved Gag precursors MA-CA-NC to the transducer, as depicted in Scheme 1 A. Treatment of the sur-

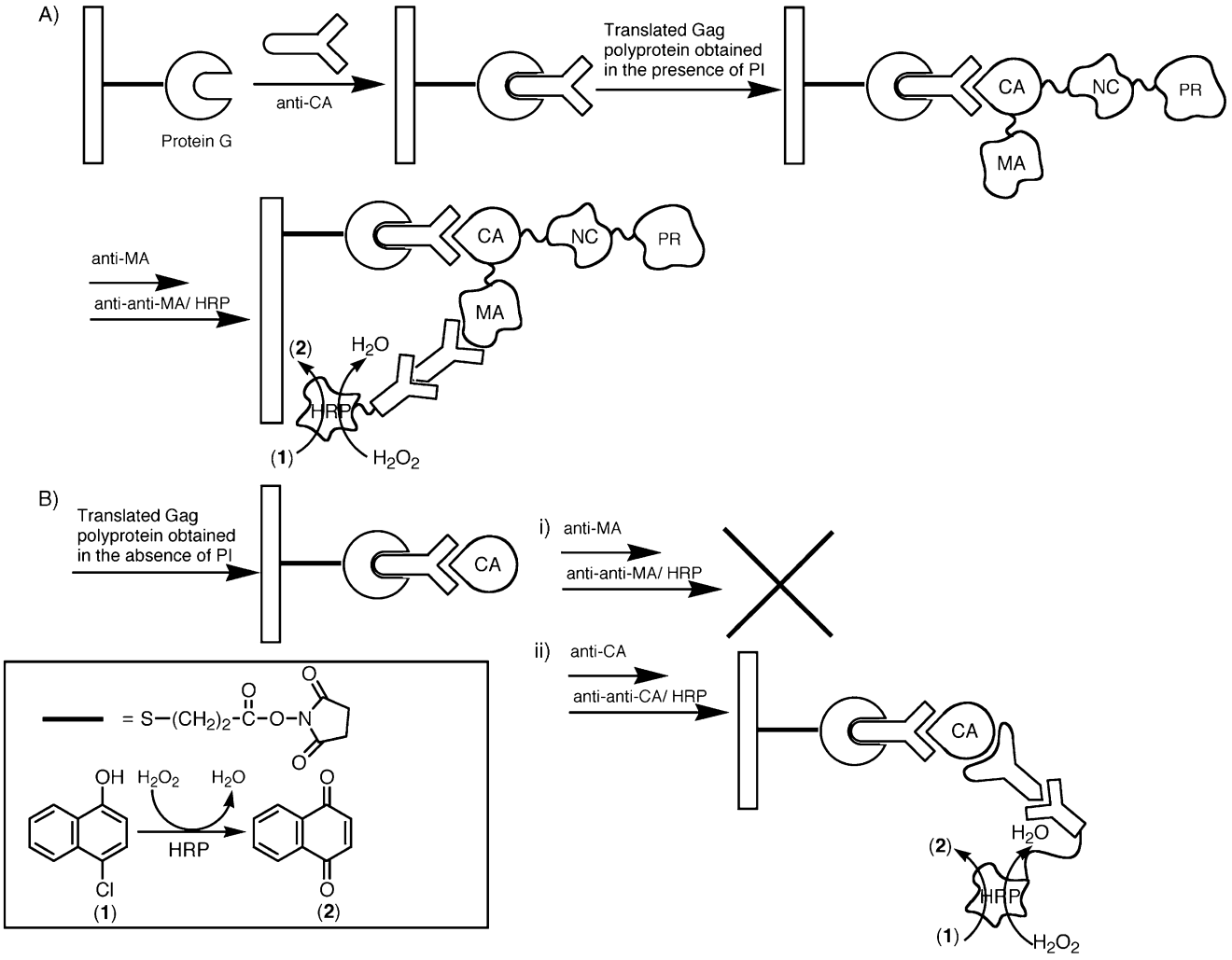

Scheme 1. *Bioelectronic transduction of translated HIV-1 Gag polyproteins. A) Analysis of MA in the translated proteins obtained in the presence of the PI. B) Detection of MA (route i) and CA (route ii) in the translated Gag polyproteins obtained in the absence of PI.*

face with the anti-MA-Ab results in antibody association to the MA fragment. Further binding of the secondary anti-MA anti-Ab/HRP conjugate to the assembly, followed by the biocatalyzed H_2O_2-mediated oxidation of 4-chloronaphthol (**1**) to the precipitate (**2**), amplifies primary recognition of the uncleaved Gag precursor assembly. On the other hand, a fully functional protease cleaves the precursor, and the MA-CA site is cleaved off (Scheme 1 B). Under these conditions, the CA fragment binds to the sensing interface, but the anti-MA antibody and the secondary anti-Ab/HRP conjugate do not associate with the transducer, so the biocatalyzed precipitation of **2** is retarded, as in Scheme 1 B, route i) (provided that nonspecific adsorption processes are minimized). The PR inhibition is thus assayed through the biocatalyzed precipitation of **2** on the electrode or the Au–quartz crystal by using Faradaic impedance spectroscopy or microgravimetric quartz crystal microbalance measurements, respectively (for the physical background of the methods, vide infra). Note that the extent of precipitation is governed by the inhibition efficiency of the translated PR, and that as the inhibitory effect decreases, the accumulation of **2** on the transducers is reduced. It should also be noted that the detection of the nonhydrolyzed Gag polyprotein is a consequence of two amplification steps. In the first step, the translation of the viral RNA to the protein provides an amplification path. The second amplification step involves the biocatalyzed precipitation of **2** on the transducers. As a single recognition event of the nonhydrolyzed polyprotein by the anti-CA sensing interface is translated into the accumulation of many insoluble molecules on the transducer, the precipitation process represents an effective amplification route. To confirm the formation of the anti-CA-Ab/CA complex in the system that includes the functional PR, the resulting interface is allowed to react with another anti-CA-Ab, and the secondary anti-CA anti-Ab/HRP conjugate is then linked to the surface. The biocatalytic interface catalyzes the precipitation of **2**, as shown in Scheme 1 B, route ii). The formation of the precipitate on the electronic transducer is probed by electrochemical means (Faradaic impedance spectroscopy) or by microgravimetric quartz crystal microbalance measurements. The development of the bioelectronic schemes for analysis of HIV-1 drug resistance was carried out in the following phases: i) assessment of viral RNA extracted from bacteria expressing viral proteins in the presence and in the absence of the PR inhibitor, ii) the assessment of viral RNA extracted from cells infected by wild-type HIV-1 or by a drug-resistant HIV-1 mutant in the absence or in the presence of the PR inhibitor, and iii) the assessment of RNA extracted from blood samples of AIDS patients by the synthesis of the viral proteins in the absence or in the presence of the PR-inhibitor. The method enables us to assess the relative amounts of drug-resistant PR, as well as relative concentrations of inhibitors required to inhibit PR.

Impedance spectroscopy is an effective method for probing the features of surface-modified electrodes.[33] The complex impedance can be presented as the sum of the real—$Z_{re}(\omega)$—and imaginary—$Z_{im}(\omega)$—components, originating mainly from the resistance and the capacitance of the electrode interface, respectively. Modification of the metallic surface with a biomaterial or an organic layer decreases the double-layer capacitance and retards the interfacial electron-transfer kinetics. The electron-transfer resistance at the electrode is given by Equation (1), where R_{Au} and R_{mod} are the electron-transfer resistance of the unmodified electrode and the variable electron-transfer resistance introduced by the modifier, in the presence of the solubilized redox probe, respectively. A typical shape of a Faradaic impedance spectrum (presented in the form of a Nyquist plot, Z_{im} versus Z_{re} at variable frequencies) includes a semicircle region lying on the Z_{re} axis followed by a straight line. The semicircle portion, observed at higher frequencies, corresponds to the electron-transfer-limited process, whereas the linear part is characteristic of the lower frequency range and represents the diffusion-limited electron-transfer process. The diameter of the semicircle corresponds to the electron-transfer resistance at the electrode surface, R_{et}.

$$R_{et} = R_{Au} + R_{mod} \quad (1)$$

The precipitation of the insoluble product on the electrode support can also be probed by microgravimetric quartz crystal microbalance (QCM) analyses.[34] The analysis of the Gag polyproteins as in Scheme 1 involves the binding of the proteins to the sensing interface, followed by the association of the detecting antibody and the anti-Ab/enzyme conjugate. These binding processes alter the mass on the piezoelectric crystal. The subsequent biocatalyzed precipitation of **2** on the crystal represents a time-dependent mass change occurring on the transducer. The frequency change of a quartz crystal (Δf) resulting from a mass alteration on the crystal (Δm) is given by the Sauerbrey equation [Eq. (2)], where f_o is the resonance frequency of the quartz crystal, A is the piezoelectrically active area, ρ_q is the density of quartz (2.648 g cm^{-3}), and μ_q is the shear modulus (2.947×10^{11} dyn cm^{-2} for AT-cut quartz).

$$\Delta f = -2 f_o^2 \frac{\Delta m}{A(\mu_q \rho_q)^{1/2}} \quad (2)$$

Figure 1 shows the Faradaic impedance spectra that correspond to the build-up of the sensing interface and to the analysis of the in vitro translation of the total bacterial RNA in the presence of saquinavir, according to Scheme 1 A. The redox label in the electrolyte solution is $Fe(CN)_6^{3-}/Fe(CN)_6^{4-}$. The electron-transfer barrier (resistance) to the redox label, resulting from the formation of the protein layers and the biocatalytic generation of the insoluble product on the electrode surface, is employed to probe the translation process. The stepwise association of protein G and the anti-CA-Ab results in an increase in the electron-transfer resistances at the electrode surface to 200 and 400 Ω (curves a and b), respectively. This increase in the interfacial electron-transfer resistances is attributable to the partial hydrophobic insulation of the electrode support by the proteins. Parallel microgravimetric QCM analyses indicate that the surface coverage of protein G is about 8.8×10^{-11} mol cm^{-2} and of anti-CA-Ab about 2.0×10^{-12} mol cm^{-2}. Binding of the Gag polyprotein through CA to the anti-CA-Ab further increases the interfacial electron-transfer resistance to

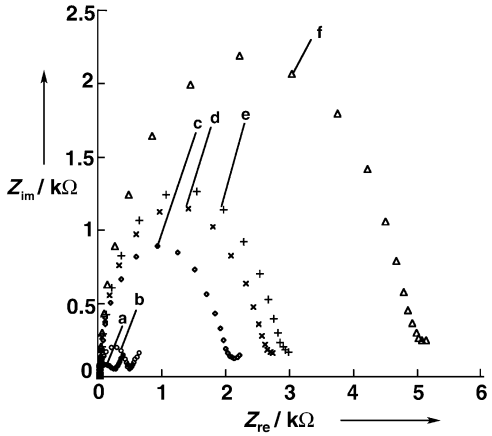

*Figure 1. Faradaic impedance spectra (depicted in the form of Nyquist plots, Z_{im} versus Z_{re}) that follow the construction of the sensing interface and the analysis of the MA Gag polyprotein translated from bacterial RNA in the presence of the PI (saquinavir, 1×10^{-4} M). a) The protein G-modified Au electrode. b) After the immobilization of anti-CA onto the surface. c) After the association of the translated Gag polyprotein. d) After the binding of anti-MA to the surface. e) After the association of the anti anti-MA/HRP conjugate. f) After the biocatalyzed precipitation of **2** in the presence of **1** (1×10^{-3} M) and H_2O_2 (1.5×10^{-4} M) for a time interval of 10 min. Data were recorded in a 0.1 M phosphate buffer solution (pH 7.0) containing $Fe(CN)_6^{3-/4-}$ (1×10^{-2} M) as redox label. The electrode was biased at 0.175 V versus SCE, and an alternating voltage (10 mV) in the frequency range of 100 mHz to 10 kHz was applied.*

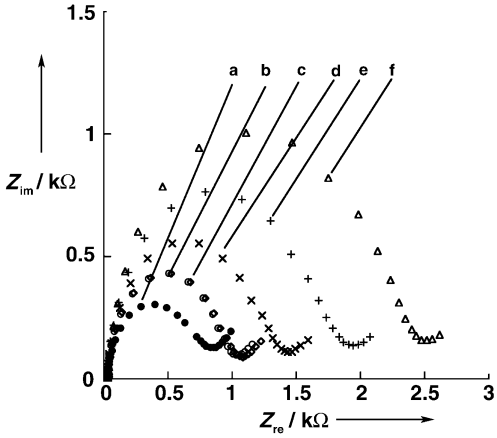

*Figure 2. Faradaic impedance spectra (Nyquist plots) corresponding to the analysis of the MA units in the translated Gag polyprotein from bacterial RNA obtained in the absence of the PI. a) The protein G-modified electrode. b) After the association of the anti-CA. c) After binding of the translated product. d) After the association of anti-MA. e) After the linkage of anti anti-MA/HRP. f) After the biocatalyzed precipitation of **2** in the presence of **1** (1×10^{-3} M) and H_2O_2 (1.5×10^{-4} M). Experimental details are similar to those detailed in Figure 1.*

2100 Ω (curve c). The association of the anti-MA antibody to the interface increases the interfacial electron-transfer resistance to $R_{et}=2800\ \Omega$ (Figure 1, curve d); the increase in the interfacial electron-transfer resistances upon the association of the Gag polyprotein and anti-MA-Ab is consistent with the association of the proteins insulating the electrode surface and perturbing the interfacial electron transfer to the redox label solubilized in the electrolyte solution. Upon addition of the anti-anti-MA-HRP conjugate we observe a further increase in the electron-transfer resistance to $R_{et}=3000\ \Omega$ (Figure 1, curve e). The subsequent biocatalyzed precipitation of **2** results in a significant increase in the interfacial electron-transfer resistance ($R_{et}=5000\ \Omega$; Figure 1, curve f), indicating that an amplified detection of the Gag polyprotein is indeed observed, and implying that inhibition of the protease in the Gag precursor did indeed occur.

Figure 2 shows the Faradaic impedance spectra obtained upon the conduction of the in vitro translation of the Gag polyprotein in the absence of the PR inhibitor. This experiment enables us to probe the protease activity according to Scheme 1 B, route i). Curve a shows the spectrum observed upon the attachment of protein G to the surface of an Au electrode, curve b depicts the spectrum obtained upon attachment of the Fc fragment of the anti-CA antibody to the protein G on the electrode support, and curve c shows the spectrum after the attachment of the translated CA units obtained under conditions where proteolysis of the Gag precursor occurred. Curve d corresponds to the spectrum obtained after an attempt to bind the anti-MA antibody to the sensing interface, and curves e and f to the subsequent attempts to bind the anti-anti-MA/HRP conjugate and to stimulate the biocatalyzed precipitation of **2**, respectively. Interestingly, we find that upon treatment of the system with the anti-MA antibody, an increase in the interfacial electron-transfer resistance ($\Delta R_{et}\approx400\ \Omega$) is observed, implying that the antibody binds to the sensing interface even though the MA sites should not exist on the surface, due to the proteolytic activity of PR. The anti-MA-Ab associated to the interface stimulates the binding of the anti-Ab/HRP conjugate and the precipitation of the insoluble product. Note, however, that the translation of identical quantities of mRNA in the absence and in the presence of the saquinavir inhibitor yield substantially different electron-transfer resistances: while the inhibited translation yields an electrode with a high electron-transfer resistance (ca. 5100 Ω) and an increase in the interfacial electron-transfer resistance of $\Delta R_{et}\approx2000\ \Omega$ upon the precipitation of **2**, the electrode treated with the uninhibited translation mixture yields an electrode with an interfacial electron-transfer resistance of only 2500 Ω, and an increase in the interfacial electron resistance of $\Delta R_{et}=500\ \Omega$ upon the precipitation of **2**, a value four times lower than that observed for the inhibited translation mixture. The binding of the anti-MA-Ab to the sensing interface and the subsequent precipitation of **2** under conditions in which the translation of the mRNA is performed without inhibition is attributable to the existence of unprocessed polyprotein that has not been cleaved by the PR. This unprocessed polyprotein acts as a background perturbation for the analysis of the uncleaved polyprotein generated upon translation in the presence of the PI. Thus, for practical analysis of HIV-drug resistance it is mandatory to develop an analysis that assays, in parallel, the background level of unprocessed protein, and the polyprotein content generated by translation in the presence of the PI.

Although the sensing interface has a low coverage by the unprocessed polyprotein, it also includes a high content of the hydrolyzed CA units, generated in the translation mixture. This

was confirmed by analysis of the modified electrode according to Scheme 1 B, route ii) and is depicted in Figure 3. In this experiment the sensing interface consisting of the anti-CA antibody is treated with the translation mixture to "fish out" the hydrolyzed CA and residual unprocessed polyprotein (curve c).

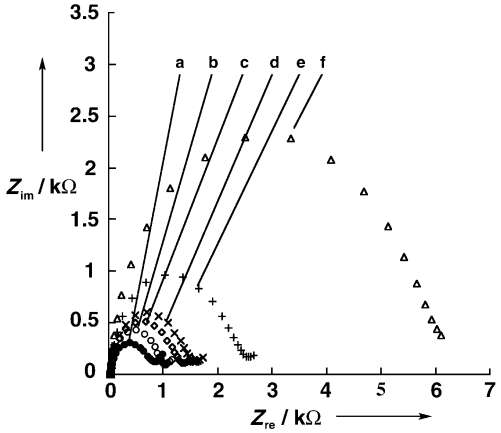

Figure 3. *Faradaic impedance spectra (Nyquist plots) corresponding to the analysis of the CA units in the translated proteins obtained from bacterial RNA in the absence of PI. a) The protein G-modified electrode. b) After the association of the anti-CA. c) After binding of the translated product. d) After the association of anti-CA. e) After binding of the anti anti-CA/HRP conjugate. f) After the biocatalyzed precipitation of* ***2*** *in the presence of* ***1*** *(1×10^{-3} M) and H_2O_2 (1.5×10^{-4} M). Experimental details as given in Figure 1.*

The increase in the interfacial electron-transfer resistance to $R_{et}=1600\ \Omega$ indicates binding of proteins to the surface. Further association of a second anti-CA-Ab and the anti-anti-CA-Ab/HRP conjugate (curves d and e, respectively), followed by the precipitation of **2**, leads to a pronounced increase in the interfacial electron-transfer resistance of the electrode to $R_{et}=6200\ \Omega$. The increase in the interfacial electron-transfer resistance as a result of the precipitation of **2** is $\Delta R_{et}\approx3600\ \Omega$. This difference is higher than the value observed upon the precipitation of **2** in the presence of the anti-MA-Ab (cf. Figure 1, $\Delta R_{et}=2000\ \Omega$) and is attributed to the higher affinity of the anti-CA-Ab as compared to the anti-MA-Ab to the respective antigens.

Microgravimetric quartz crystal microbalance experiments further confirm the results and conclusions extracted from the Faradaic impedance measurements. Table 1 summarizes the frequency changes of functionalized Au–quartz crystals upon analysis of the MA in the translated Gag polyprotein in the presence and in the absence of the PR inhibitor (saquinavir) and analysis of the CA in the translated polyprotein in the absence of the inhibitor. Total RNA from cultured cells was employed in these experiments. In all of the systems, the sensing interface consists of the protein G as base monolayer (8.8×10^{-11} mol cm^{-2}) and the associated anti-CA layer as the recognition interface. Entry (a) summarizes the frequency changes observed in stepwise analysis of the Gag polyprotein translated in the presence of the inhibitor, as in Scheme 1 A. The frequency changes ($\Delta f=-50$ Hz) observed upon treatment of the surface with the translated proteins, and also upon interaction with anti-MA ($\Delta f=-80$ Hz), indicate that an unprocessed Gag polyprotein is generated upon translation. The biocatalyzed precipitation of **2** results in a frequency change of $\Delta f=-100$ Hz, consistent with the effective formation of a precipitate on the transducer. Entry (b) summarizes the frequency changes observed upon analysis of the unprocessed Gag polyprotein in the translation mixture obtained in the absence of the inhibitor. The frequency change of -40 Hz observed upon the precipitation of **2** implies that uncleaved Gag polyprotein exists in the translation mixture, consistently with the conclusion obtained from the impedance measurements. Table 1, entry (c) summarizes the frequency changes upon analysis of the CA unit obtained upon translation in the absence of the inhibitor, as in Scheme 1 B, route ii). In this case, both the cleaved and the uncleaved CA are analyzed. The biocatalyzed precipitation of **2** results in a frequency change of -150 Hz, indicating that anti-anti-CA/HRP conjugate was associated with the sensing interface. We see that the formation of **2** in the presence of anti-CA is enhanced in relation to the effectiveness of the generation of **2** in the presence of the anti-MA. This observation is in agreement with the Faradaic impedance analyses, and may be attributed to the higher affinity of the anti-CA for the respective precursor.

The experiments described above demonstrate that we are able to transduce the differences in the translation of mRNA electronically in the presence and in the absence of the PI. Nonetheless, the method is not free of analytical limitations, due to: i) the existence of unprocessed polyprotein even in the absence of the inhibitor, ii) the difference in the anti-CA and anti-MA antibody affinities to the respective antigens, and—most importantly—iii) the difficulties involved in retaining constant mRNA concentrations in the analyzed samples. In order to overcome these limitations, we formulated the assay protocol outlined in Scheme 2. The extracted RNA sample is subdivided into two equal samples, A and B. While sample A is sub-

Table 1. *Microgravimetric quartz crystal microbalance analyses of the translated MA and CA units in the presence and in the absence of the saquinavir PR inhibitor.*[a]

	Anti-MA Δf [Hz]	Anti-CA Δf [Hz]	Anti-anti-MA/HRP Δf [Hz]	Anti-anti-CA/HRP Δf [Hz]	Precipitation of **2** Δf [Hz]
a) Translated Gag polyprotein in the presence of PR inhibitor	−80	–	−140	–	−100
b) Translated Gag polyprotein in the absence of PR inhibitor	−15	–	−30	–	−40
c) Translated proteins in the absence of PR inhibitor	–	−150	–	−110	−150

[a] Frequency changes are determined at time intervals identical to the impedance measurements.

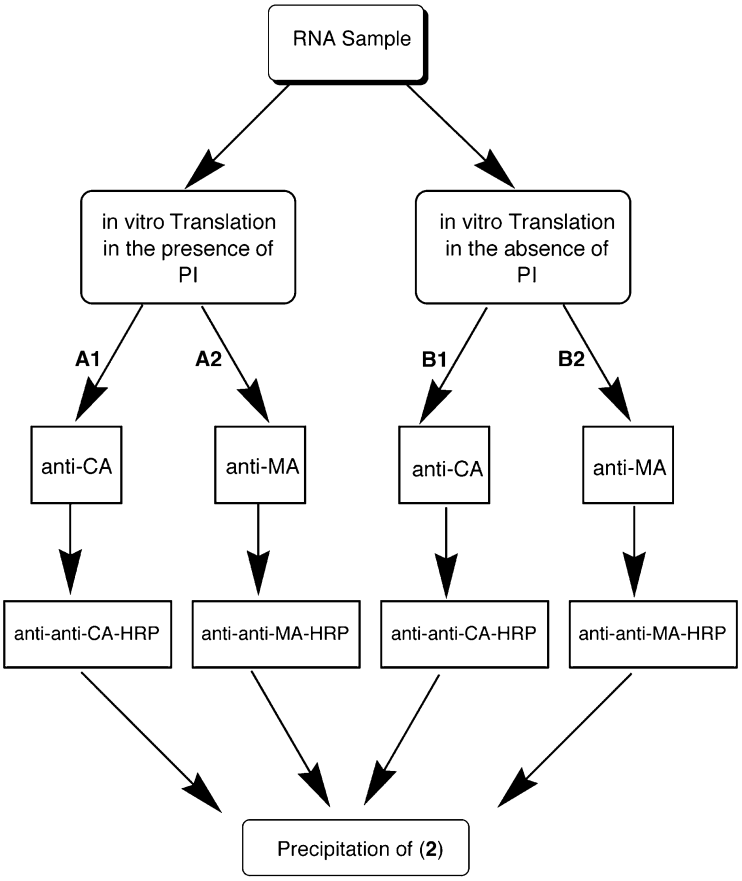

Scheme 2. *Analytical protocol for the determination of PI resistance in AIDS patients.*

jected to the in vitro translation in the presence of the PI, sample B is translated in the absence of the PI. Each of the translation mixtures is then further divided into two equal sub-samples: A1 and A2, and B1 and B2, respectively. The samples A1 and B1 are subjected to analysis of the total CA units by use of anti-CA, according to Scheme 1 B, route ii). The samples A2 and B2 utilize the anti-MA antibody to assess the polyprotein contents in the respective samples, according to Scheme 1 A and B, route i). Note that the ratio of the interfacial electron-transfer resistances generated upon the precipitation of **2** in routes A2 and B2 reflect the content of polyprotein generated under PR inhibition against the unprocessed polyprotein in the system. The ratio of the electron-transfer resistances of paths A1 and B1 should be independent of PI, and its value should be ≈ 1. This ratio provides an internal standard for the effectiveness of translations in the entire set of experiments. Thus, the four-path analysis scheme for the mRNA translation processes eliminates the background signal of unprocessed polyproteins in the absence of the inhibitor. The assay also abrogates the difference in the affinities of anti-CA and anti-MA for the respective antigens. Since the original sample is subdivided into equivalent sub-samples prior to the translations, the problem of different RNA contents in analyses paths is cancelled out.

To verify the analysis method shown in Scheme 2, we applied it to analyze the translation processes of wild-type HIV-1 in the absence and in the presence of PI, and in parallel we have analyzed the translation processes of RNA extracted from the G48V mutated virus, which is resistant to saquinavir.[35,36] Figure 4 shows the Faradaic impedance spectra corresponding to the final step of precipitation of **2** on the electrode supports after the application of the analytical protocol outlined in Scheme 2. Figure 4 A shows the spectra (curves a and b) obtained for the translation of the RNA derived from the wild-type virus in the absence of the inhibitor according to paths B1 and B2 in Scheme 2, re-

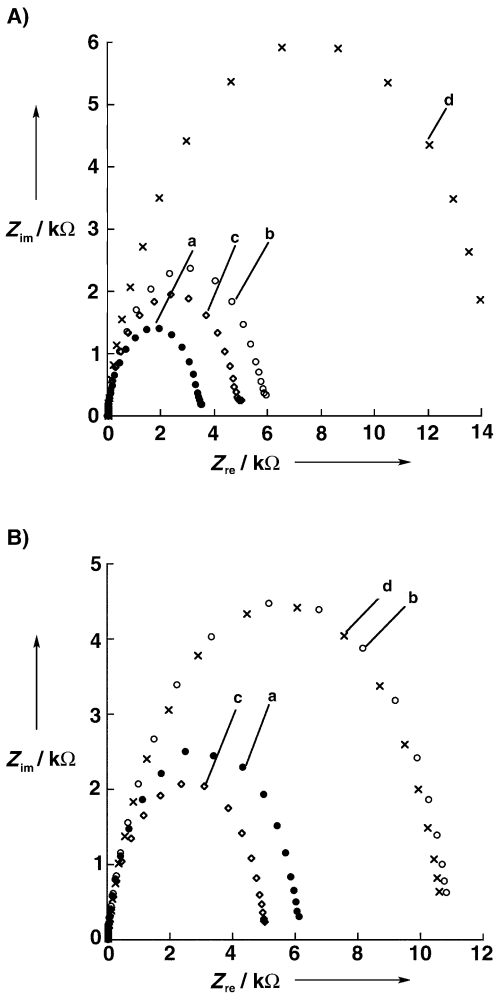

Figure 4. *A) Faradaic impedance spectra corresponding to analysis of the translated proteins obtained from the mRNA from the media of cultured cells infected by wild-type HIV-1, in the presence and absence of the PI (saquinavir, 1×10^{-4} M) according to Scheme 2. The spectra reflect the impedance responses of the electrodes after the final step of the biocatalyzed precipitation of **2** in the presence of **1** (1×10^{-3} M) and H_2O_2 (1.5×10^{-4} M) for a time interval of 10 min: a) analysis of CA in the absence of PI, b) analysis of MA in the absence of PI, c) the analysis of CA in the presence of PI, and d) analysis of MA in the presence of PI. B) Faradaic impedance spectra corresponding to the analysis of the translated proteins obtained from the mRNA from the media of cultured cells infected with the HIV-1 G48V mutant, in the presence and in the absence of PI, according to Scheme 2. The spectra depict the impedance responses of the electrodes after the final step of the biocatalyzed precipitation of **2**, in the presence of **1** (1×10^{-3} M) and H_2O_2 (1.5×10^{-4} M) for 10 min: a) analysis of CA in the absence of PI, b) analysis of MA in the absence of PI, c) analysis of CA in the presence of PI, and d) analysis of MA in the presence of PI.*

spectively. Figure 4A, curves c and d are the Faradaic impedance spectra observed for the Au electrodes in analysis of the translation mixture of the wild-type HIV obtained in the presence of saquinavir as the PI, according to paths A1 and A2, respectively. As expected, the electron-transfer resistance for the inhibited virus analyzed with anti-MA for the uncleaved protein according to path A2 is the higher and corresponds to $R_{et}=$ 14 kΩ. For comparison, the use of the anti-MA for analysis of the uninhibited protease encoded by the wild-type viral RNA according to path B2 yields an electron-transfer resistance of $R_{et}=6$ kΩ. Clearly, the ratio of electron-transfer resistances of the inhibited vs. uninhibited wild-type HIV is $R_{et}^{B2}/R_{et}^{A2}=0.43$. An identical analysis scheme was applied to analyze the saquinavir-resistant mutated HIV-1^{G48V}. Figure 4B, curves b and d show the parallel analyses of the translation processes of RNA extracted from the G48V mutant according to paths B2 (without inhibitor) and A2 (with inhibitor), respectively. The resulting interfacial resistances in the two systems are identical ($R_{et}\approx$ 11 kΩ), indicating no effect of the inhibitor on the protease activity. The ratio $R_{et}^{B2}/R_{et}^{A2}=1$ is observed for the G48V system, as expected. Note, however, that we observe a difference in the electron-transfer resistances resulting from analysis of the wild-type virus according to path B2 ($R_{et}=6$ kΩ) as compared to the HIV-1^{G48V} analyzed by path B2 ($R_{et}=11$ kΩ). This implies that the protease activities of the wild-type virus and of the HIV-1^{G48V} differ, and that the PR of the mutant has a lower activity for processing (hydrolyzing) the polyprotein.

The method outlined in this study has enabled us to develop a quantitative assay to probe the effect of inhibitor concentration on the activity of the viral PR. Since the interfacial electron-transfer resistance analyzed according to Scheme 1A directly translates into the content of uncleaved Gag polyprotein, the interfacial electron-transfer resistance correlates with the inhibition efficiency of the translated PR activity by the specific inhibitor. Figure 5 shows the calibration curve corresponding to the interfacial electron-transfer resistances of electrodes used for analysis of the Gag polyproteins translated from the RNA of HIV-1 infected cultured cells, in the presence of increased concentrations of the saquinavir inhibitor. Clearly, as the concentration of the saquinavir increases, the interfacial electron-transfer resistance is enhanced, consistently with the elevated uncleaved Gag polyprotein content. Such quantitative correlation between the inhibitor concentration and the uncleaved polyprotein content should be of extreme importance for determination of drug doses and drug efficiencies.

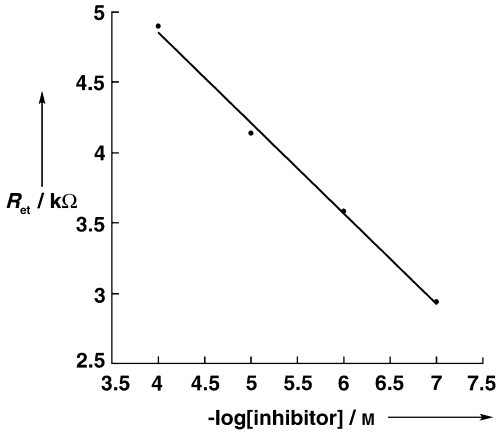

Figure 5. *Calibration curves corresponding to the analysis of the MA units in the unprocessed Gag polyprotein obtained from the translation of RNA from cultured cells infected with HIV-1, in the presence of variable concentration of the PI (saquinavir). The calibration curve depicts the observed interfacial electron-transfer resistances after the biocatalyzed precipitation of* ***2*** *upon analysis of the MA units according to Scheme 1A.*

Finally, the analysis scheme outlined in Scheme 2 was applied to detection of drug resistance in AIDS patients treated with saquinavir. In this process, it is to be expected that analysis of the CA units by the anti-CA antibodies should lead to an electron-transfer resistance ratio corresponding to $\alpha=R_{et}^{A1}/R_{et}^{B1}\approx 1.0$ for paths B1 and A1, whereas the ratio of electron-transfer resistance on analysis of the MA units with the anti-MA antibody should show a value of $\beta=R_{et}^{B2}/R_{et}^{A2}\approx 1.0$ for drug-resistant patients, whereas $\beta=R_{et}^{B2}/R_{et}^{A2}<1$ should be observed for non-drug-resistant patients. Table 2 summarizes the results observed for five patients. From these values we were able to predict that patients #2 and #5 had developed drug resistance. It is difficult to verify the validity of these conclusions, and we have to rely on the subjective statements of the physicians who treated the patients. On the basis of this information, patients #2 and #5 were indeed suffering from severe conditions that did not react to the treatment with saquinavir, whereas all other patients were under balanced conditions. Furthermore, the results shown in Table 2 suggest that patient #1 had developed partial resistance to the drug, and this patient will be followed up by our analytical procedure in the future.

Table 2. *Analysis of HIV patients for saquinavir drug resistance.*[a]

Patient	$\alpha=R_{et}^{A1}/R_{et}^{B1}$	$\beta=R_{et}^{B2}/R_{et}^{A2}$
1	0.85 ± 0.03	0.87 ± 0.04
2	0.93 ± 0.03	1.1 ± 0.04
3	0.96 ± 0.03	0.75 ± 0.04
4	0.91 ± 0.03	0.79 ± 0.04
5	1.0 ± 0.03	1.07 ± 0.04

[a] Analyzed according to Scheme 2.

Conclusion

This study describes a rapid assay of HIV patients for drug resistance. The method is based on measurement of the resistance phenotype of the HIV-1 protease through the in vitro translation of HIV-1 viral mRNA extracted from the patient in the absence and in the presence of the HIV-1 PR-inhibiting drug saquinavir and comparison of the PR activity in the two different translation paths. A major accomplishment of the study is the successful analysis of the corresponding proteins generated by the minute amounts of mRNA extracted from the blood samples. This success derives from the amplification

routes involved in the detection scheme: i) the translation process represents a biocatalytic amplification, and ii) the biocatalyzed precipitation of (**2**) represents a biocatalytic amplification that follows a few recognition events on the electrode. The analysis scheme for detection of the HIV-1 drug resistance is relatively rapid and efficient and, under nonoptimized, nonautomatic conditions, approximately five to six samples could be analyzed by a single operator within 24 h. The method should be applicable for analysis of any HIV-1 PI, and should also enable assessment of the effectiveness of prescribed drugs, as well as drug doses.

Experimental Section

Chemicals: IgG-goat-anti-rabbit-horseradish peroxidase (HRP), IgG-goat-anti-mouse-HRP (anti-Ab-HRP), hydrogen peroxide, 4-chloro-1-naphthol, 3,3′-dithiodipropionic acid bis(*N*-hydroxysuccinimide) (DSP) active ester, protein G, and the other chemicals were from commercial sources (Aldrich or Sigma) and were used as supplied without further purification. Monoclonal mouse IgG-anti-CA was contributed by Dr. K. Steimer and obtained through the AIDS Research and Reference Reagent Program, Division of AIDS, NIAID, NIH. Polyclonal rabbit IgG-anti-MA was prepared by immunization of rabbits with purified recombinant MA protein. The biotin in vitro translation kit was purchased from Roche Diagnostics, Mannheim (Germany). The PR inhibitor saquinavir (Ro 31–8959)[37] was a gift from Roche Products, and was initially dissolved in 10% dimethyl sulfoxide (DMSO) to a concentration of 1.0 mM and stored at −20 °C until further use. Ultrapure water from Elgastat (VHQ) source was used throughout this work.

Characterization and pretreatment of electrodes: Gold wire electrodes (0.5 mm diameter, ≈0.2 cm^2 geometrical area, roughness coefficient ≈1.2–1.5) were used for the electrochemical measurements. To remove any previous organic layer, and to regenerate a bare metal surface, the electrodes were treated in a boiling solution of KOH (2 M) for 4 h, and were then rinsed with water and stored in concentrated sulfuric acid. Prior to modification, the electrodes were rinsed with water, dried, and soaked for 2 min in fresh piranha solution (30% H_2O_2, 70% H_2SO_4). The resulting electrodes were then rinsed with water, soaked for 10 min in concentrated nitric acid, and again rinsed with water.

Electrochemical measurements: A conventional three-electrode cell, consisting of the modified Au electrode, a glassy carbon auxiliary electrode isolated by a glass frit, and a saturated calomel electrode (SCE) connected to the working volume with a Luggin capillary, was used for the electrochemical measurements. The cell was positioned in an earthed Faraday cage. Impedance measurements were performed with an electrochemical impedance analyzer (EG&G, model 1025) and potentiostat (EG&G, model 283) connected to a computer (EG&G Software Power Suite 1.03 for impedance measurements). All electrochemical measurements were performed in phosphate buffer (0.1 M, pH 7.0) as a background electrolyte solution. Faradaic impedance measurements were performed in the presence of a $K_3[Fe(CN)_6]/K_4[Fe(CN)_6]$ (10 mM) mixture (1:1) as a redox probe. Impedance measurements were performed at a bias potential of 0.175 V versus SCE with alternating voltage (10 mV) in the frequency range of 100 mHz to 10 kHz. The impedance spectra were plotted in the form of complex plane diagrams (Nyquist plots).

Microgravimetric measurements: A QCM analyzer (Fluke 164T multifunction counter, 1.3 GHz, TCXO) linked to a personal computer and a homemade flow cell with a working volume of 0.3 mL was employed. Quartz crystals (AT-cut, 9 MHz, EG&G) sandwiched between two Au electrodes (area 0.196 cm^2, roughness factor ≈3.5) were used. The Au–quartz crystals were cleaned with a piranha solution, followed by rinsing with water.

Electrode modifications: The electrodes were rinsed with water, dried, and soaked in a solution of the DSP-active ester (10 mM) in DMSO for 30 min at room temperature. The functionalized electrodes were rinsed with DMSO and water and incubated in a solution of protein G (100 μg mL^{-1}) for 90 min in a phosphate buffer saline solution (pH 7.4) at room temperature, to couple protein G lysine residues covalently to the functionalized electrodes. The protein G-functionalized electrodes were then allowed to interact with the Fc fragment of the anti-CA antibody (1 μg mL^{-1}) for 30 min at room temperature to yield the sensing interfaces.

Analytical procedure: The antibody-functionalized electrode was treated with varying concentrations of the Gag polyprotein generated in the translation mixture for 60 min, diluted to 1.0 mL with phosphate-buffered saline (PBS) solution (pH 7.0) at room temperature. After attachment of the respective polyprotein to the sensing interface, the electrode was incubated in the solution of anti-MA or anti-CA (sources were diluted 200-fold) for 30 min at room temperature. After attachment to the respective antibody, the electrode was incubated either in a goat-anti-rabbit-HRP conjugate (2.5 μg mL^{-1}) for the MA analysis, or in a goat-anti-mouse-HRP conjugate (2.5 μg mL^{-1}) for the CA analysis, for 30 min at room temperature. 4-Chloro-1-naphthol (**1**) was dissolved initially in ethanol and the ethanolic stock solution was then diluted with phosphate buffer (0.1 M, pH 7.0) to yield the developing solution containing **1** (1 mM) and ethanol (2% *v/v*). The modified (HRP-tagged antibody-functionalized) electrodes were incubated in the developing solution of **1** for a fixed time of 10 min at room temperature to stimulate the precipitation of **2**. After incubation of the electrodes in the probe solution, they were rinsed with phosphate buffer (0.1 M, pH 7.0) and introduced into the electrochemical cell for analysis by Faradaic impedance spectroscopy. It should be noted that the electrode was rinsed thoroughly with buffer solution (pH 7.0) after each step, to eliminate any unspecific adsorbates on the electrode. In the microgravimetric quartz crystal microbalance measurements, the various modification and amplification steps, including the rinsing steps, were performed in the flow cell of the QCM apparatus.

Cells and viruses: Sup T1 cells were maintained in RPM1 1640 medium supplemented with 10% fetal calf serum, antibiotics (penicillin and streptomycin), and glutamine (2 mM). HIV-1_{IIIB} infect (kindly supplied by Dr. Wainberg, Lady Davis Institute, Montreal, Canada) was used to infect the cultured cells at 0.1 multiplicity of inspection (MOI), and virus was harvested 7–9 days post infection. Culture medium containing the virus was clarified from cell debris by centrifugation at 10000 rpm for 10 min and the clear supernatant was centrifuged for 45 min at 45000 rpm in a Beckman centrifuge (SW 50.1 rotor). The drug-resistant HIV-1 (NL4-3) strain that includes the G48V mutated PR was constructed and propagated as described previously.[36]

Blood samples: Plasma was obtained from consenting donors, with removal of blood cells by centrifugation for 5 min at 3000 rpm. The plasma was diluted threefold with PBS, and viral particles were pelleted by centrifugation of the volume for 45 min at 45000 rpm in a Beckman centrifuge (SW 50.1 rotor). The viral pellets were suspended in TRIzol reagent (1 mL, Gibco BRL) con-

taining tRNA (5–10 μg, Sigma) as carrier and RNA was extracted according to the manufacturer's instructions.

In vitro translation: All RNA preparations were translated in vitro by use of a "Biotin in vitro translation kit" (Roche 1559951) in the absence or in the presence of saquinavir (Ro 31-8959). Reactions were performed in 50 μL, according to the manufacturer's instructions, with use of DEPC-treated water. The PR inhibitor saquinavir was dissolved in NaCl (1 M) in the DEPC-treated water, and was added to reaction mixtures before the start of the synthesis. The reaction mixtures were incubated for 90 min at 30 °C, and the reactions were halted by placing on ice or storage at −75 °C until further use.

Acknowledgements

L.A. acknowledges the Levi Eshkol fellowship, Israel Ministry of Science. Parts of the research were supported by an Infrastructure Project, Israel Ministry of Science (I.W.) and by the Israel Science Foundation (M.K.), and performed in the Peter A. Krueger Laboratory, with the generous support of Nancy and Lawrence Glick and Pat and Marvin Weiss.

Keywords: biosensors · drug resistance · electronic transduction · HIV · inhibitors

[1] K. Hertogs, S. Bloor, S. D. Kemp, C. Van den Eynde, T. M. Alcorn, R. Pauwels, M. Van Houtte, S. Staszewski, V. Miller, B. A. Larder, *Aids* **2000**, *14*, 1203.
[2] J. Garcia-Lerma, W. Heneine, *J. Clin. Virol.* **2001**, *21*, 197.
[3] U. Nillroth, L. Vrang, P. O. Markgren, J. Hulten, A. Hallberg, U. H. Danielson, *Antimicrob. Agents Chemother.* **1997**, *41*, 2383.
[4] N. T. Parkin, Y. S. Lie, N. Hellmann, M. Markowitz, S. Bonhoeffer, D. D. Ho, C. J. Petropoulos, *J. Infect. Dis.* **1999**, *180*, 865.
[5] J. M. Coffin, *Science* **1995**, *267*, 483.
[6] J. L. Meynard, M. Vray, L. Morand-Joubert, E. Race, D. Descamps, G. Peytavin, S. Matheron, C. Lamotte, S. Guiramand, D. Costagliola, F. Brun-Vezinet, F. Clavel, P. M. Girard, *Aids* **2002**, *16*, 727.
[7] N. Koch, C. Tamalet, N. Tivoli, J. Fantini, N. Yahi, *J. Clin. Virol.* **2001**, *21*, 153.
[8] T. Jacks, H. D. Madhani, F. R. Masiarz, H. E. Varmus, *Cell* **1988**, *55*, 447.
[9] M. A. Navia, P. M. Fitzgerald, B. M. McKeever, C. T. Leu, J. C. Heimbach, W. K. Herber, I. S. Sigal, P. L. Darke, J. P. Springer, *Nature* **1989**, *337*, 615.
[10] S. Crawford, S. P. Goff, *J. Virol.* **1985**, *53*, 899.
[11] I. Katoh, Y. Yoshinaka, A. Rein, M. Shibuya, T. Odaka, S. Oroszlan, *Virology* **1985**, *145*, 280.
[12] N. E. Kohl, E. A. Emini, W. A. Schleif, L. J. Davis, J. C. Heimbach, R. A. Dixon, E. M. Scolnick, I. S. Sigal, *Proc. Natl. Acad. Sci. USA* **1988**, *85*, 4686.
[13] N. Almog, R. Roller, G. Arad, L. Passi-Even, M. A. Wainberg, M. Kotler, *J. Virol.* **1996**, *70*, 7228.
[14] M. Kotler, G. Arad, S. H. Hughes, *J. Virol.* **1992**, *66*, 6781.
[15] G. Zybarth, H. G. Krausslich, K. Partin, C. Carter, *J. Virol.* **1994**, *68*, 240.
[16] J. H. Condra, D. J. Holder, W. A. Schleif, O. M. Blahy, R. M. Danovich, L. J. Gabryelski, D. J. Graham, D. Laird, J. C. Quintero, A. Rhodes, H. L. Robbins, E. Roth, M. Shivaprakash, T. Yang, J. A. Chodakewitz, P. J. Deutsch, R. Y. Leavitt, F. E. Massari, J. W. Mellors, K. E. Squires, R. T. Steigbigel, H. Teppler, E. A. Emini, *J. Virol.* **1996**, *70*, 8270.
[17] J. H. Condra, C. J. Petropoulos, R. Ziermann, W. A. Schleif, M. Shivaprakash, E. A. Emini, *J. Infect. Dis.* **2000**, *182*, 758.
[18] S. G. Deeks, M. Smith, M. Holodniy, J. O. Kahn, *JAMA* **1997**, *277*, 145.
[19] I. Willner, B. Willner, *Trends Biotechnol.* **2001**, *19*, 222.
[20] K. Habermuller, M. Mosbach, W. Schuhmann, *Fresenius J. Anal. Chem.* **2000**, *366*, 560.
[21] I. Willner, E. Katz, *Angew. Chem.* **2000**, 112, 1230; *Angew. Chem. Int. Ed.* **2000**, *39*, 1180.
[22] B. Koenig, M. Graetzel, *Anal. Chim. Acta* **1995**, *309*, 19.
[23] A. B. Kharitonov, J. Wasserman, E. Katz, I. Willner, *J. Phys. Chem. B* **2001**, *105*, 4205.
[24] G. Wittstock, H. Emons, W. R. Heineman, *Electroanalysis* **1996**, *8*, 143.
[25] E. M. Boon, D. M. Ceres, T. G. Drummond, M. G. Hill, J. K. Barton, *Nature Biotechnol.* **2000**, *18*, 1096.
[26] S. O. Kelley, E. M. Boon, J. K. Barton, N. M. Jackson, M. G. Hill, *Nucleic Acids Res.* **1999**, *27*, 4830.
[27] Y. Okahata, Y. Matsunobu, K. Ijiro, M. Mukae, A. Murakami, K. Makino, *J. Am. Chem. Soc.* **1992**, *114*, 8299.
[28] L. Alfonta, I. Willner, D. J. Throckmorton, A. K. Singh, *Anal. Chem.* **2001**, *73*, 5287.
[29] F. Patolsky, Y. Weizmann, I. Willner, *J. Am. Chem. Soc.* **2002**, *124*, 770.
[30] F. Patolsky, A. Lichtenstein, I. Willner, *J. Am. Chem. Soc.* **2001**, *123*, 5194.
[31] F. Patolsky, K. T. Ranjit, A. Lichtenstein, I. Willner, *Chem. Commun.* **2000**, 1025.
[32] F. Patolsky, A. Lichtenstein, M. Kotler, I. Willner, *Angew. Chem.* **2001**, 113, 2321; *Angew. Chem. Int. Ed.* **2001**, *40*, 2261.
[33] A. J. Bard, L. R. Faulkner in *Electrochemical Methods: Fundamentals and Applications*, Wiley, New York, **1980**.
[34] A. Janshoff, H. J. Galla, C. Steinem, *Angew. Chem.* **2000**, 112, 4164; *Angew. Chem. Int. Ed.* **2000**, *39*, 4004.
[35] S. I. Wilson, L. H. Phylip, J. S. Mills, S. V. Gulnik, J. W. Erickson, B. M. Dunn, J. Kay, *Biochim. Biophys. Acta* **1997**, *1339*, 113.
[36] I. Blumenzweig, L. Baraz, A. Friedler, U. H. Danielson, C. Gilon, M. Steinitz, M. Kotler, *Biochem Biophys. Res. Commun.* **2002**, *292*, 832.
[37] N. A. Roberts, J. A. Martin, D. Kinchington, A. V. Broadhurst, J. C. Craig, I. B. Duncan, S. A. Galpin, B. K. Handa, J. Kay, A. Krohn, R. W. Lambert, J. H. Merrett, J. S. Mills, K. E. B. Parkes, S. Redshaw, A. J. Ritchie, D. L. Taylor, G. J. Thomas, P. J. Machin, *Science* **1990**, *248*, 358.

Received: January 15, 2004

